



PERGAMON

Scripta Materialia 46 (2002) 187–192



www.elsevier.com/locate/scriptamat

Crystallization kinetics of an amorphous TiAl sheet produced by PVD

O.N. Senkov^{b,*}, M.D. Uchic^a, S. Menon^b, D.B. Miracle^a

^a Air Force Research Laboratory, Materials and Manufacturing Directorate, AFRL/MLLMD, Wright-Patterson AFB, OH 45433-7817, USA

^b UES, Inc., 4401 Dayton-Xenia Road, Dayton, OH 45432-1894, USA

Received 3 September 2001; received in revised form 11 October 2001; accepted 6 November 2001

Abstract

An amorphous, 150 μm thick freestanding sheet of a TiAl-based alloy was produced by a physical vapor deposition method. The following phase transformations were observed and analyzed using differential thermal analysis and X-ray diffraction, amorphous \rightarrow body centered cubic $\beta \rightarrow$ hexagonal close-packed $\alpha \rightarrow$ tetragonal γ + ordered HCP α_2 . © 2002 Acta Materialia Inc. Published by Elsevier Science Ltd. All rights reserved.

Keywords: Physical vapor deposition; Differential thermal analysis; X-ray diffraction; Amorphous materials; Titanium aluminide; Phase transformations

1. Introduction

Titanium aluminides are considered as promising materials for use in sheet form for high-temperature aerospace applications such as thermal protection systems because of their low density, high temperature strength, reasonable oxidation resistance, and low thermal conductivity [1]. However, these materials are generally brittle at temperatures below 700 °C, which may cause fracturing and failure of the thermal protection system. The ductility of TiAl alloys can be improved through microstructural modifications. In particular, the brittle-to-ductile transition temper-

ature can be decreased and ductility can be improved by grain refinement to submicron-size levels [2–4]. Non-equilibrium processes such as rapid solidification, mechanical alloying, or physical vapor deposition can be effectively used to produce fine-grain structures. Moreover, it has recently been established that TiAl-based alloys can become amorphous when produced by these non-equilibrium techniques [5–9]. The amorphous phase can then be a precursor to a nanocrystalline structure by simultaneous compaction and crystallization through control of the time and temperature conditions [9]. Of course, knowledge of the crystallization kinetics of the amorphous phase and microstructural evolution of crystallized phases is required to properly control the final microstructure and properties.

In the present work, an amorphous sheet of a TiAl-based alloy was produced by physical vapor

* Corresponding author. Tel.: +1-937- 255-1320; fax: +1-937-656-7292.

E-mail address: oleg.senkov@wpafb.af.mil (O.N. Senkov).

deposition (PVD), and the crystallization kinetics of the amorphous phase were studied during continuous heating. The phases produced after crystallization and their lattice parameters were also identified.

2. Experimental procedures

A freestanding film of a γ -TiAl alloy was deposited using a magnetron sputtering method. A Ti-46.5Al-2Nb-1.6Cr-0.5W (atomic %) alloy of potential engineering importance [10] was used as the target material. The film was deposited onto a 50 mm \times 75 mm polished Cu substrate, using a 152 mm diameter sputtering gun with a source-to-substrate distance of 100 mm. During deposition, the substrate temperature was held to below 40 °C using a water-cooled substrate holder, and the substrate temperature was monitored using a thermocouple in intimate contact with the substrate. The chamber base pressure was better than 2×10^{-7} Torr prior to deposition, and high-purity Ar gas was flowed through the chamber at a rate of 80 sccm and a pressure of 3 mTorr during deposition. For the deposition, a DC power supply was kept at constant power of 500 W, and the target was sputtered for 1 h prior to starting the deposition run. The deposition lasted for 48 h, which resulted in a film thickness of approximately 150 μ m. Freestanding foils were obtained by removing the as-deposited substrate from the vacuum chamber, at which time the γ -TiAl film spontaneously delaminated from the substrate.

Crystallization kinetics of the amorphous phase were studied using a Universal V2.3C TA differential thermal analysis (DTA) unit. The samples were heated in the temperature range of 50–1000 °C in an argon atmosphere. Heating rates of 5, 10, 20, 30 and 50 °C/min were used to determine the activation enthalpy of the processes controlling crystallization and phase transformations in this temperature range by Kissinger's method [11]. Microstructural characterization was performed on foils heated to selected temperatures at the rate of 5 °C/min and then immediately cooled at a rate exceeding 20 °C/min. The phases present in the specimens were examined via X-ray diffraction

(XRD) with the use of a Rigaku Rotaflex X-ray diffractometer, using CuK_α radiation.

3. Results

An XRD pattern of the TiAl-based alloy produced by PVD is shown in Fig. 1(a). A spread halo is present in the 2θ range of 35–45°, indicating that the sheet was fully amorphous. Transmission electron microscopy of the as-deposited film shows an amorphous matrix with a small volume fraction (<1 vol.%) of a crystalline phase, which is illustrated in Fig. 2. DTA shows three exothermic reactions in the temperature range of 50–1000 °C during heating at a rate of 5 °C/min, with reaction maxima at 523, 537, and 648 °C, as shown in Fig. 3. To understand the origin of these reactions, the as-deposited foils were heated in the DTA at the rate of 5 °C/min to 520, 530, 575 or 800 °C (corresponding locations on the DTA curve are shown in Fig. 3), immediately cooled after reaching these temperatures and analyzed with the use of XRD. The XRD patterns of the heat-treated specimens are given in Fig. 1(b)–(e).

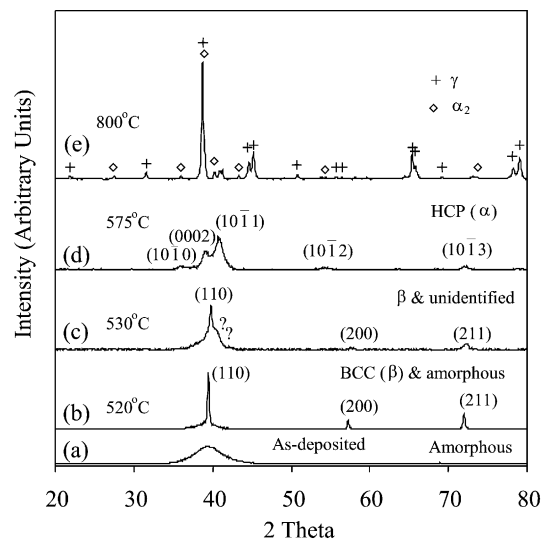


Fig. 1. XRD patterns of a TiAl foil produced by PVD in (a) as-deposited condition and (b)–(e) after heating at (b) 520 °C, (c) 530 °C, (d) 575 °C and (e) 800 °C.

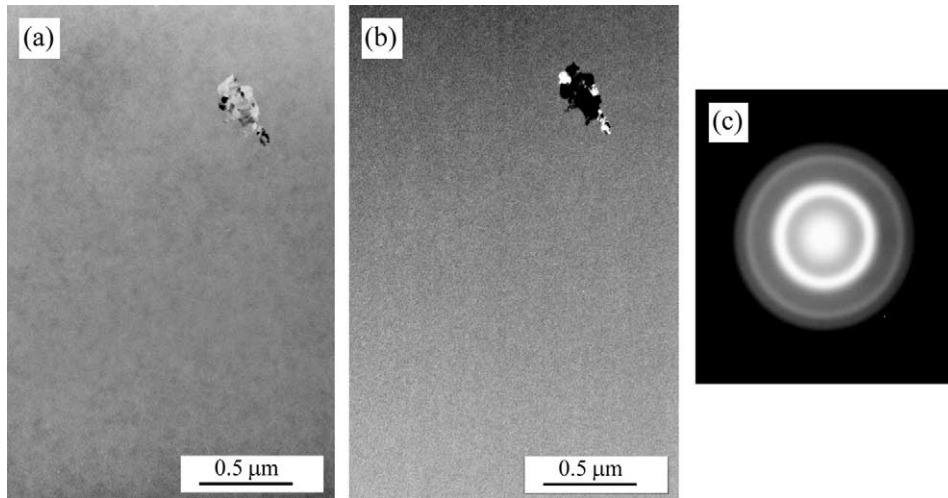


Fig. 2. (a) Bright-field and (b) dark-field TEM images of the as-deposited TiAl sheet and (c) corresponding selected area diffraction pattern. The volume fraction of small crystallites, which have been identified as the HCP α_2 phase, inside the amorphous phase is <1%.

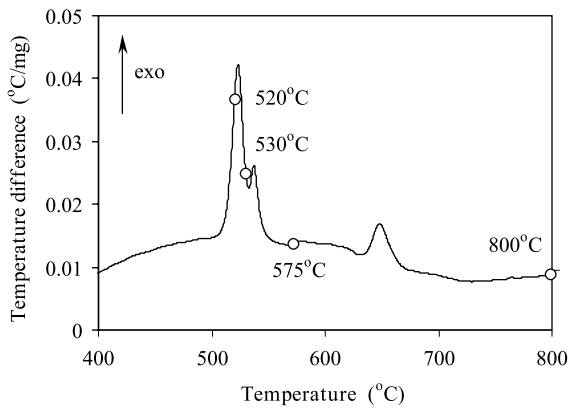


Fig. 3. DTA curve of an amorphous TiAl sheet produced by PVD. Heating rate is 5 °C/min. Characteristic points of the DTA curve to which several specimens were heated for the following XRD analysis are indicated by open circles and the corresponding temperatures are given.

After heating to 520 °C (i.e. 3 °C below the maximum for the first exothermic reaction), three intense peaks from a crystalline phase together with a halo from a residual amorphous phase are detected, Fig. 1(b). These three peaks identified a body centered cubic (BCC, β) phase with the lattice parameter $a = 0.3195$ nm. This β phase was also present after heating to 530 °C, and two additional peaks from an unidentified crystalline

phase were also detected on the XRD pattern from this specimen (see Fig. 1(c)).

Heating the specimen to 575 °C, i.e. above the second exothermic reaction but below the third one (Fig. 3) resulted in the XRD pattern shown in Fig. 1(d). No amorphous halo was detected and the wide XRD peaks were identified as belonging to the disordered hexagonal close packed (HCP) α phase, with the lattice parameters $a = 0.289$ nm and $c = 0.460$ nm. Intensities of the XRD peaks from this phase were much smaller and the peaks were wider as compared to the XRD peaks from the BCC (β) phase, which may indicate that the grains of the α phase were much finer than the grains of the β phase. Recent TEM studies [12] also support this statement.

After heating to 800 °C, i.e. above the third exothermic reaction shown in Fig. 3, two phases were easily identified on the corresponding XRD pattern (Fig. 1(e)). These are the ordered HCP α_2 phase and the tetragonal γ phase. The XRD peaks from the latter phase were much more intense than those from the α_2 phase, indicating that the γ phase was the major phase in this annealed specimen. The lattice parameters of the γ phase were determined to be $a = 0.4008$ nm and $c = 0.4055$ nm, and the lattice parameters of the α_2 phase were $a = 0.578$ nm and $c = 0.460$ nm.

It can be concluded from the DTA and XRD results described above that during continuous heating of the TiAl-based amorphous sheet at a heating rate of 5 °C/min, crystallization of the amorphous phase initiates at 513 °C with a formation of a metastable BCC β phase. The metastable β phase is present only in a very narrow temperature range, and it transforms into the α phase (through formation of an unidentified metastable phase) at a temperature range of 530–545 °C. The produced α phase has a very fine grain size, which is manifested by broad, low-intensity XRD peaks and has been confirmed in a recent TEM investigation [12]. This phase is also metastable in the temperature range studied, and it transforms into the γ and ordered α_2 phases in the temperature range of 637–670 °C.

Fig. 4 shows the effect of the heating rate on the kinetics of crystallization and phase transformations in the PVD TiAl-based sheet. All reactions shift towards higher temperatures when the heating rate increases. However, the magnitudes of the peak shifts are different for the three reactions. Further, the first and second peaks become superimposed at heating rates of 20 °C/min and higher. As a result, the amorphous phase crystallizes directly to the α phase, without intermediate formation of the β phase, when the heating rate exceeds 20 °C/min.

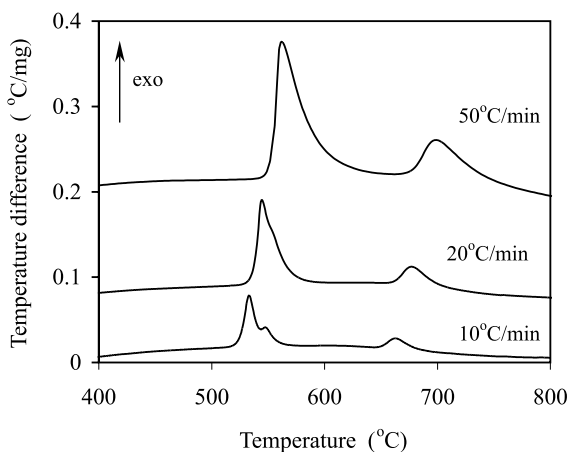


Fig. 4. DTA curves of an amorphous TiAl sheet produced by PVD. The heating rates of 10, 20 and 50 °C/min are shown near corresponding DTA curves.

According to Kissinger [11], the activation energy, E , of the process controlling the transformation is given by the following equation:

$$E = -R \frac{d[\ln(v/T_p^2)]}{d(1/T_p)} \quad (1)$$

where v is the heating rate, T_p is the peak maximum temperature, and R is the gas constant. Therefore, the activation energy can be determined from slopes of the curves $\ln(v/T_p^2)$ versus $1/T_p$. These curves are plotted in Fig. 5 for each of the three exothermic reactions, showing linear dependency. The activation energies were determined for the first, second and third exothermic peaks to be 315 ± 5 kJ/mol (for amorphous to β), 363 ± 20 kJ/mol (for β to α), and 324 ± 5 kJ/mol (for α to α_2 and γ), respectively. These values can be compared with the activation energies for self-diffusion in β -Ti (250 kJ/mol) [13] and α -Ti (193 kJ/mol) [14], volume interdiffusion in α_2 (312 kJ/mol) and γ (295 kJ/mol) phases [15], and volume diffusion of Ti in the γ phase (291 kJ/mol) [16].

The values of self-diffusion in α -Ti and β -Ti are too low to provide agreement with the measured activation energies. Further, diffusion in elemental Ti is not likely to represent a relevant physical process in the current alloys with high Al con-

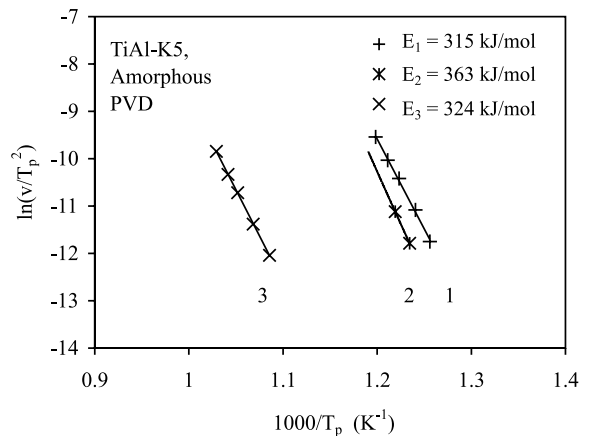


Fig. 5. Dependencies of the logarithm of the heating rate (in K/min) normalized to the square of the peak temperature T_p on the reciprocal peak temperature for the first, second and third exothermic peaks. The activation energies calculated from the corresponding slopes are given in the plot area.

centrations. As the first two transformations established here represent reactions that are far from equilibrium, they may be difficult to relate to physical processes that have been characterized in equilibrium crystalline structures. On the other hand, the measured activation energy of 324 kJ/mol for the transformation from α to $\gamma + \alpha_2$ in the present study is within 10% of the values cited for volume diffusion in α_2 (312 kJ/mol) and γ (295 kJ/mol), and for Ti diffusion in γ (291 kJ/mol). Each of these mechanisms are possible rate-limiting reactions for this final transformation; however, the current measurements are unable to distinguish between these three possible mechanisms.

The transformation from the amorphous structure to α and then from α to γ and α_2 phases were accounted for in an earlier study of amorphous TiAl-based alloys prepared by mechanical alloying [9,17]; however, higher temperatures of the transformations were reported than were shown in our work. The difference in the results may be due to contamination of the mechanically alloyed powder with interstitial elements, which may stabilize the amorphous phase. No formation of the BCC β phase during crystallization of an amorphous phase was previously reported in this alloy system. It should be noted that only one heating rate of 20 °C/min was used in [9,17], and we have shown that the β phase cannot be detected at this high heating rate (see Fig. 4).

A metastable primitive cubic phase [6] or a tetragonal phase [7] was detected using TEM during crystallization of an amorphous phase in TiAl foils produced by magnetron sputtering. The tetragonal phase was observed only in very thin regions of TEM specimens and only during in situ experiments at temperatures above 600 °C [7], and might be due to contamination of these regions with oxygen or carbon. The primitive cubic phase, similar to β -Mn and with the lattice parameter $a = 0.69$ nm, was discovered in thicker foils annealed at 527 °C for 1 h [6]. It is interesting that two diffraction peaks from an unidentified phase were detected in our work (see Fig. 1(c)), after annealing at almost the same temperature. Analysis showed that these two unidentified peaks may be interpreted as the most intense (2 2 1) and (3 1 0) lines of the primitive cubic phase with the lattice

parameter $a = 0.67$ nm. However, we have not positively identified this phase at this time. Detailed results of investigation of microstructure and mechanical properties of the alloy at different stages of crystallization will be reported elsewhere.

4. Conclusions

1. An amorphous, freestanding sheet of a TiAl-based alloy was produced by physical vapor deposition methods using a pre-alloyed target, and the sheet thickness was approximately 150 μm .
2. The amorphous phase is stable at temperatures up to ~ 510 °C, and at higher temperatures, crystallization occurs in two stages. At heating rates below 20 °C/min, a metastable BCC (β) phase, stable only within a very narrow (≈ 10 °C) temperature range, is initially formed, which then transforms into an HCP (α) phase (through formation of another metastable phase, probably with a primitive cubic structure). At higher heating rates, the amorphous phase transforms directly into the α phase, without formation of the β phase.
3. The metastable α phase transforms into a mixture of stable tetragonal (γ) and ordered α_2 phases at temperatures above about 640 °C by an exothermic reaction.
4. Activation energies of the processes responsible for the transformations, amorphous $\rightarrow \beta$, $\beta \rightarrow \alpha$ and $\alpha \rightarrow (\gamma + \alpha_2)$, were determined to be 315 ± 5 , 363 ± 20 , and 324 ± 5 kJ/mol, respectively.

Acknowledgements

The authors want to thank Dr. D.M. Dimiduk for discussion of the results and valuable comments and Dr. R. Wheeler, Mr. A. Smith, and Mr. T. Houston, of UES Inc., for help in specimen preparation and characterization. The work was conducted under AFRL contract no. F33615-01-C-5214.

References

- [1] Chan KS, Kim YW. *Acta Metall Mater* 1995;43:439.
- [2] Semiatin SL, Seetharaman V, Weiss I. *Mater Sci Eng* 1998;A243:1.
- [3] Imaev RM, Salishchev GA, Imaev VM, Shagiev MR, Kuznetsov AV, Senkov ON, Froes FH. *Mater Sci Eng* 2001;A300:263.
- [4] Imaev VM, Imaev RM, Kuznetsov AV, Senkov ON, Froes FH. *Mater Sci Technol* 2001;17:566.
- [5] Shao G, Grosdider T, Tsakiroopoulos P. *Scripta Metall Mater* 1994;30:809.
- [6] Abe E, Ohnuma M, Nakamura M. *Acta Mater* 1999;47:3607.
- [7] Banerjee R, Swaminathan S, Wheeler R, Fraser HL. *Phil Mag A* 2000;80:1715.
- [8] Ameyama K, Okada O, Hirai K, Nakabo N. *Metall Trans JIM* 1995;36:269.
- [9] Senkov ON, Srisukhumbowornchai N, Ovecoglu ML, Froes FH. *J Mater Res* 1998;13:3399.
- [10] Kim YW. *JOM* 1994;46(7):30.
- [11] Kissinger HE. *Anal Chem* 1957;29:1702.
- [12] Senkov ON, Uchic M, Miracle DB. Unpublished work. 2001.
- [13] Nakajima H, Koiwa M. *ISIJ Int* 1991;31:757.
- [14] Herzig C, Willicke P, Vierregge K. *Phil Mag A* 1991;63:949.
- [15] Sprengel W, Nakajima H, Oikawa H. *Mater Sci Eng A* 1996;A213:45.
- [16] Kroll S, Mehrer H, Stolwijk N, Herzig C, Rozenkranz R, Frommeyer G. *Z Metallkunde* 1992;83:591.
- [17] Senkov ON, Srisukhumbowornchai N, Froes FH. In: *Value Addition Metallurgy*. Warrendale: TMS; 1998. p. 61.